Arch. Met. Geoph. Biokl., Ser. A, 28, 39–52 (1979)

ARCHIV
FÜR METEOROLOGIE
GEOPHYSIK UND
BIOKLIMATOLOGIE

551.509.313

National Research Institute for Mathematical Sciences of the CSIR, Pretoria, South Africa

ADI Solution of the Inverse Balance Equation Over a Non-Rectangular Region

I. M. Navon

With 6 Figures

Received July 28, 1978

Summary

A Poisson-type equation arising in a commonly used numerical weather forecasting model is solved using an alternating direction implicit (ADI) method with Wachpress optimum parameters on a trapezoidal domain which coincides with the operational forecast domain.
Various optimum parameter sequences were obtained for the corresponding squares which enclose the region under consideration, computational efficiency being the criterion which determined the choice of the particular parameter sequence finally selected.
In regard to accuracy and computational efficiency, results over several forecast days using the ADI method were compared with those obtained using the successive over-relaxation (SOR) method. It turned out that for a 48 × 29 grid the ADI method was nearly three times as fast as the optimum SOR method.

Zusammenfassung

ADI-Lösung der inversen Bilanzgleichung über einer nicht-rechteckigen Region

Eine in einem allgemein verwendeten Modell der numerischen Wettervorhersage gebrauchte Gleichung vom Poisson-Typ wird mit Hilfe der ADI-Methode mit optimalen Parametern nach Wachpress auf einem trapezoidförmigen Gebiet, das mit dem Vorhersagebereich zusammenfällt, gelöst.
Verschiedene Folgen von optimalen Parametern wurden für die entsprechenden Quadrate, die die in Betracht gezogene Region einschließen, erhalten, wobei die Leistungsfähigkeit der Berechnungsmethode das Kriterium war, das die Auswahl der schließlich gewählten besonderen Parameterfolge bestimmte.
Hinsichtlich Genauigkeit und Leistungsfähigkeit der Berechnungsmethode wurden die für einige Tage mit der ADI-Methode erhaltenen Ergebnisse mit den mit der SOR-Methode erhaltenen Ergebnissen verglichen. Es ergab sich, daß für ein Netz von 48 × 29 Gitterpunkten die ADI-Methode nahezu dreimal so schnell zum Ergebnis führt wie die beste SOR-Methode.

0066-6416/79/0028/0039/$ 02.80

1. Introduction

Owing to its simplicity, the point SOR iterative method has been the most popular of the iterative methods employed for solving the Poisson equation in problems of computational fluid dynamics [8].
In SOR methods, however, the number of iterations required for convergence increases with N, the number of mesh divisions of the space dimension, while when ADI methods [6] are applied to square regions the number of iterations required for convergence is almost independent of N [1], so that when N is large enough, ADI methods are preferable (see, for example [1, 10]).
No guidelines are available for non-rectangular geometries, as in this case the theory on which the determination of an ADI parameter sequence is based no longer applies [4, 9]. Nevertheless, parameter sequences obtained for the smallest square which encloses the region under consideration are often used, and rapid convergence of the iteration procedure is achieved [4, 3, 12].
It is the aim in this paper to introduce and apply such a method to a Poisson-type equation arising in numerical weather forecasting when the domain is not rectangular, but trapezoidal in shape.
In Section 2 the Poisson-type equation which represents an inverse balance equation is described, along with the region on which it is to be solved. Finite-difference expressions are derived for the differential operator appearing in the equation.
The ADI algorithm is introduced in Section 3, along with the Wachpress' method for obtaining a sequence of optimum iteration parameters. The embedding-square method is then introduced.
Finally, in Section 4, numerical solutions are discussed of the inverse balance equation for several forecast days, obtained using the ADI and SOR methods. Isolines of the solution height field z for the 600 mb surface pressure are plotted on the operational weather forecast maps for solution based on both the ADI and the SOR methods.

2. The Inverse Balance Equation

2.1 Basic Equations

List of symbols:

$d = \Delta x = \Delta y$	grid interval
m	map magnification factor from earth to plane $= \dfrac{1 + \sin 60^\circ}{1 + \sin \phi} = 1.866/(1 + \sin \phi$
a	mean radius of the earth

r	radial distance of the particle as measured from the centre of the earth
ϕ	latitude
r_n	ADI iteration parameters
z	height of the 600 mb pressure surface
f	Coriolis parameter
ψ	stream function
ρ, ρ_E	parameters of the stereographic projection (see Fig. 1)
x, y	coordinates of the stereographic projection plane
I	identity matrix

In the operational numerical weather forecasting model commonly in use at some meteorological services [7, 13] a Poisson-type equation arises whenever an inverse balance equation is to be solved, i. e. when the geopotential height field z is to be derived from the stream function for rotational wind component field $v = k \times \nabla \psi$.
The general inverse balance equation can be written as

$$g\nabla^2 z = \nabla(f\nabla\psi) + 2\left[\frac{\partial^2\psi}{\partial x^2}\frac{\partial^2\psi}{\partial y^2} - \left(\frac{\partial^2\psi}{\partial x\,\partial y}\right)^2\right] \tag{1}$$

if the stereographic projection coefficients are ignored; if, on the other hand, they are taken into account, the most general form of the inverse balance equation is

$$\begin{aligned} m^2 g(z_{xx} + z_{yy}) + \tfrac{1}{2} f^2 = {} & \tfrac{1}{2}[m^2(\psi_{xx} + \psi_{yy} + f]^2 - \\ & - \frac{m^4}{2}\left[\psi_{xx} - \psi_{yy} + \frac{4\rho}{\rho_E^2 + \rho^2}\cdot\frac{x\psi_x - y\psi_y}{\rho}\right]^2 - \\ & - \frac{m^4}{2}\left[2\psi_{xy} + \frac{4\rho}{\rho_E^2 + \rho^2}\cdot\frac{x\psi_y - y\psi_x}{\rho}\right]^2 + m^2\left[\psi_y f_y + \psi_x f_x - \frac{1}{r^2}(\psi_x^2 + \psi_y^2)\right] \end{aligned} \tag{2}$$

The strem function ψ is known, and we therefore have a Poisson equation for z, the height field.

2.2 Trapezoidal Integration Domain

The Northern Hemisphere is mapped onto a polar stereographic projection true at 60°N, for which the map factor is $m = 1.866/(1 + \sin\phi)$. The operational forecast domain is a rectangle inside the stereographic projection, extending from latitude 10°N to 90°N and longitude 100°W to 95°E. The area is covered by a 48 × 29 horizontal grid system which gives a grid size of $\Delta x = \Delta y = 381$ km at 60°N.

Owing to the low value of the Coriolis parameter south of 10°N and also the scarcity of observations in that area, two triangular sections of the lower right-hand and lower left-hand corners of the rectangle are excluded from the domain of integration (Fig. 2). Thus the domain is not rectangular but trapezoidal.

The North Pole is located at grid point (27,22) while the sloping boundaries introduced in this way consist of two straight segments passing through the grid points (1,11) to (11,1) and (1,35) to (14,38) respectively.

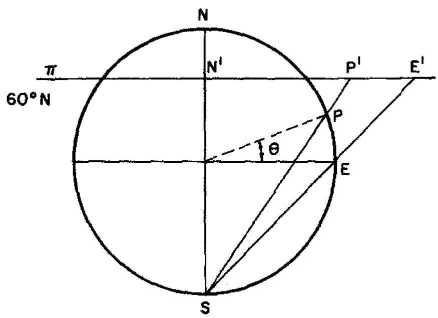

$\rho = \overline{N'P'}$

$\rho_E = \overline{N'E'}$

$$m = \frac{1 + \sin 60}{1 + \sin \theta} = \frac{\rho^2 + \rho_E^2}{2 \rho_E r}$$

Fig. 1. The polar stereographic projection

2.3 Finite-Difference Operators

For the sake of consistency with the direct Monge-Ampére type balance equation, the standard five-point finite-difference Laplacian was used for $\nabla^2 \psi$ and $\nabla^2 z$, i. e.

$$\nabla^2 z_{ij} = [z_{i+1,j} + z_{i-1,j} + z_{i,j+1} + z_{i,j-1} - 4 z_{i,j}]/d^2 \tag{3}$$

where we adopt the notation

$$z_{ij} = z(i\,\Delta x,\, j\,\Delta y) \tag{4}$$

and $d = \Delta x = \Delta y$.

The "Monge-Ampére" term $\psi_{xx}\,\psi_{yy} - \psi^2_{xy}$ was computed with an interval length $\sqrt{2}\cdot d$, i. e.

$$\psi_{xx}\psi_{yy}-\psi_{xy}^2 = \frac{1}{4d^4}\,[\psi_{i+1,j+1}-2\,\psi_{ij}+\psi_{i-1,j-1})\cdot$$

$$\cdot(\psi_{i-1,j+1}-2\,\psi_{ij}+\psi_{i+1,j-1})-(\psi_{i+1,j}+\psi_{i-1,j}-\psi_{i,j+1}-\psi_{i,j-1})^2\,]. \tag{5}$$

Centered finite differences were used for the first derivatives to maintain an $O(h^2)$ truncation error. An auxiliary contour of points (a false boundary) was introduced to hand boundary conditions of fixed z and ψ.

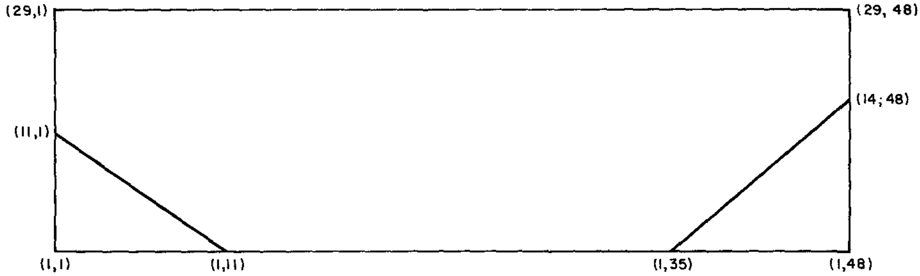

Fig. 2. The trapezoidal domain of integration

3. The ADI Iterative Algorithm

3.1 ADI Solution of the Poisson Equation for Rectangular Domains

Eq. (2) can be written in the general form

$$\nabla^2 z = f(x, y). \tag{6}$$

After finite-difference discretization we obtain a linear system of the form

$$A\,z = s, \tag{7}$$

where A is an $n \cdot n$ real, nonsingular matrix, z is the unknown vector, s is right-hand side known vector.

The ADI algorithm consists in splitting A in a way to be specified below, into the sum of two matrices H and V

$$A = H + V \tag{8}$$

so that the iteration procedure can be expressed in the matrix equations

and
$$\left\{\begin{aligned}\left(\frac{2}{r_{n+1}} I+H\right) z^{(k+\frac{1}{2})} &= \left(\frac{2}{r_{n+1}} I-V\right) z^{(k)}+s \\ \left(\frac{2}{r_{n+1}} I+V\right) z^{(k+1)} &= \left(\frac{2}{r_{n+1}} I-H\right) z^{(k+\frac{1}{2})}+s\end{aligned}\right. \tag{9}$$

where I is the identity matrix of order $(N-1)\cdot(N-1)$, r_n is an iteration parameter and the successive values of r are called a parameter sequence which optimize the convergence of the iterative process.
The solution of eqs. (9) involves solving two systems of equations having a tridiagonal coefficient matrix for each iteration sweep.
When the Laplace operator is approximated by a five-point difference scheme, the H matrix includes horizontal coupling (along lines of constant y-value) while the V matrix includes all vertical coupling (along lines of constant x-value).
The ADI algorithm for the Poisson equation

$$\nabla^2 z_{ij} = g_{ij}, \tag{10}$$

where g is the load function, takes the form:

$$\begin{aligned} &z_{i-1,j}^{(k+\frac{1}{2})}+(2-1/r_n)\,z_{ij}^{k+\frac{1}{2}}+z_{i-1,j}^{(k+\frac{1}{2})} = -z_{i,j-1}^{k}+(-2-1/r_n)z_{i,j}^{k}-z_{i,j-1}^{k}+g_{i,j}'d^2 \\ &z_{i,j-1}^{(k+1)}+(-2-1/r_n)\,z_{ij}^{(k+1)}+z_{i,j+1}^{(k+1)} = -z_{i-1,j}^{(k+\frac{1}{2})}+(2-1/r_n)\,z_{i,j}^{(k+\frac{1}{2})}-z_{i+1,j}^{(k+\frac{1}{2})}+g_{i,j}^{r}\,d^2 . \end{aligned} \tag{11}$$

The space increment is $d=\Delta x=\Delta y$ and the typical internal point is $z(i\,\Delta x, j\,\Delta y)=z_{ij}$.
For a discretized rectangular domain comprising $M\cdot N$ grid points, the H and V matrices are of order $((M-1)\cdot(N-1))$ and it can be shown that

$$H=\begin{bmatrix} C & & & 0 \\ & C & & \\ & & \ddots & \\ 0 & & & C \end{bmatrix}, \quad V=\begin{bmatrix} 2J & -J & & & 0 \\ -J & 2J & -J & & \\ & \ddots & \ddots & \ddots & \\ 0 & & -J & 2J & -J \\ & & & -J & 2J \end{bmatrix}, \tag{12}$$

with C a matrix of order $(M-1)$ given by

$$C = \begin{bmatrix} 2 & -1 & & & 0 \\ -1 & 2 & -1 & & \\ & \ddots & \ddots & \ddots & \\ & & -1 & 2 & -1 \\ 0 & & & -1 & 2 \end{bmatrix} \tag{13}$$

and J the unit matrix of order $(M-1)$.
The vectors z and g in eq. (10) are given by

$$\{z_{1,1}, \ldots, z_{1,N-1};\ z_{2,1}, \ldots, z_{2,N-1}; \ldots;\ z_{M-1,1}, \ldots, z_{M-1,N-1}\}^T \tag{14}$$

$$\{g'_{1,1}, \ldots, g'_{1,N-1};\ g'_{2,1}, \ldots, g'_{2,N-1}; \ldots;\ g'_{n-1,1}, \ldots, g'_{M-1,N-1}\}^T . \tag{15}$$

The components of the vector g' arise from the load function g and from the boundary values.

3.2 Optimum Iteration Parameters

For our problem we shall use the parameter sequence given by Wachpress [10, 11]:

$$r_{n+1} = \frac{1}{2\cos^2\left(\frac{\pi}{2M}\right)} \left(\cot^2\left(\frac{\pi}{2M}\right)\right)^{n/(n_0-1)} \quad (n = 0, 1, \ldots, n_0-1) \tag{16}$$

where $n_0(> 2)$ is the smallest integer such that

$$(\sqrt{2} - 1)^{(n_0-1)} \leqslant \tan \frac{\pi}{2M} , \tag{17}$$

M being the number of grid points in the square with side $L = Md$.

For a rectangle with sides $L_1 = M_1 d$ and $L_2 = N_1 d$ we set $M = \max(N_1, M_1)$. For the details of the derivation of this parameter sequence see [10].
The ADI iteration process is terminated when at the end of one iteration cycle consisting of n_0 ADI iterations with n_0 different iteration parameters r_n, $n = 1, 2, \ldots, n_0$, the error in eq. (18) is within the desired range of accuracy for all the points of the discretized forecast domain.
In our case the values of the height field for the 600 mb surface vary around

the mean value of 5.10^3 m and the required maximum error is 4 m, i. e. the iteration process will terminate whenever

$$|z_{ij}^{(s+1)} - z_{ij}^{(s)}| < 4 \quad \text{for all} \quad i = 1, \ldots, M, j = 1, \ldots, N \tag{18}$$

s being the number of full ADI iteration cycles.

3.3 Embedding Method for Non-Rectangular Domains

For non-rectangular domains the matrices H and V (eq. (12)) no longer commute and consequently the theory on which the determination of a parameter sequence is based no longer applies.

Mouradoglou [5] and Crowder and Dalton [2] have done some preliminary work on ADI convergence properties in a non-rectangular mesh. Parameter sequences can, however, still be obtained for the smallest square within which the region under consideration can be enclosed (see [3, 4]). Numerical experiments were conducted using various embedding squares for the trapezoidal domain, the sides of the squares ranging from $L = \sqrt{48 \cdot 29} \cdot h \simeq 37\,d$ to $L = 50\,d$; deriving the corresponding ADI iteration parameter sequences; and applying these to the Poisson eq. (2).

It was found that optimal convergence of the iteration procedure in terms of the number $N_{tot} = s \cdot n_0$ of ADI iterations necessary to attain the required accuracy was achieved for an embedding square with side $L = 48\,d$. The number of iterations in the optical cycle was $n_0 = 5$ and the number of cycles $s = 2$.

The optimum parameter sequence derived using eq. (16) was

$$\begin{aligned}
r_1 &= (3.99571800)^{-1} \\
r_2 &= (0.72295481)^{-1} \\
r_3 &= (0.13080603)^{-1} \\
r_4 &= (0.02366705)^{-1} \\
r_5 &= (0.00428214)^{-1}.
\end{aligned}$$

The r_j were applied in a monotonically decreasing order $(r_5, \ldots, r_1)$ as suggested by Wachpress [11].

Table 1 illustrates the relationship between the number of ADI iterations N_{tot} and the number N of grid points in the side of the embedding square of side $L = Nd$. n_0 is the number of iteration parameters in an ADI iteration cycle.

Table 1

N	37	40	45	48	50
n_0	4	4	4	4	4
	5	5	5	5	5
s Number of complete ADI cycles to attain prescribed accuracy	6	5	4	4	5
	5	5	3	2	3
$N_{tot} = s \cdot n_0$ Total number of ADI iterations	24	20	16	16	20
	25	25	15	10^*_{opt}	15

4. Comparison of Results Obtained Using ADI and SOR Methods

Several experiments were conducted for various forecast days, eq. (2) on the trapezoidal domain being solved by use of the ADI iterative method of Section 3.3 and a point SOR iterative method with identical accuracy requirements.

The optimal overrelaxation factor $w_b = 1.63$ for the SOR algorithm was determined using a working procedure suggested by Wachpress [10].

The average number of SOR iterations required to attain the same accuracy oscillated around $N = 35$.

The numerical experiments were conducted at the Israeli Meteorological Service using a Sigma-5 computer.

In order to ensure that identical accuracies would be obtained, the solution height field z of the 600 mb surface pressure was plotted on the operational weather forecast maps, for both the ADI and the SOR algorithms (Figs. 3 to 6).

A perfect matching of the isohypses was obtained everywhere except near the sloping boundaries, where slightly different finite-difference approximations were used for the ADI and the point SOR algorithms.

Using for the non-rectangular trapezoidal domain the ADI algorithm with iteration parameters derived by means of the embedding approach, the computation time was found to be hardly more than one third that required for the same problem by the point SOR algorithms.

For this non-rectangular region the ADI algorithm thus retains a net superiority over the SOR method.

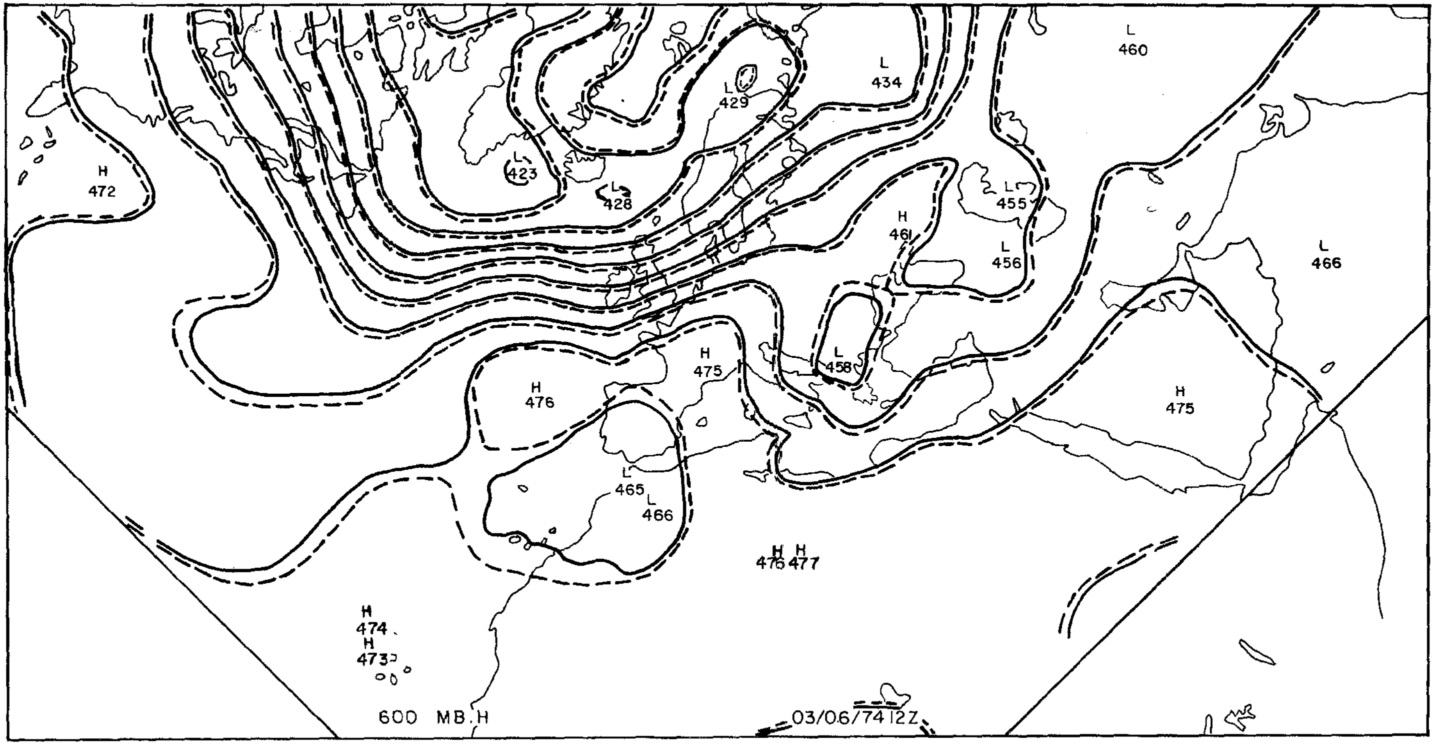

Fig. 3. 600 mb isohypse contours in dekameters for 03/06/74 12 z. Solid lines show SOR solution and dashed lines the ADI solution

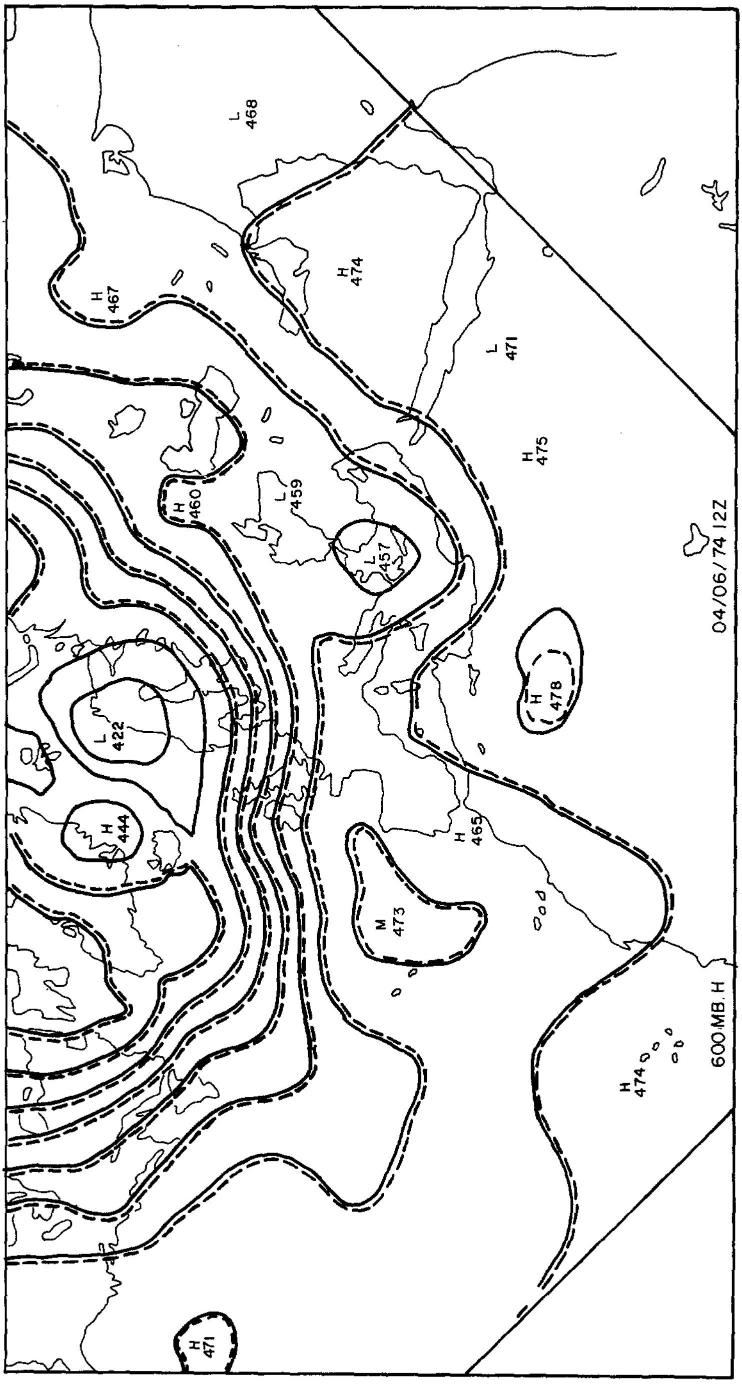

Fig. 4. 600 mb isohypse contours in dekameters for 04/06/74 12 z. Solid lines show SOR solution and dashed lines the ADI solution

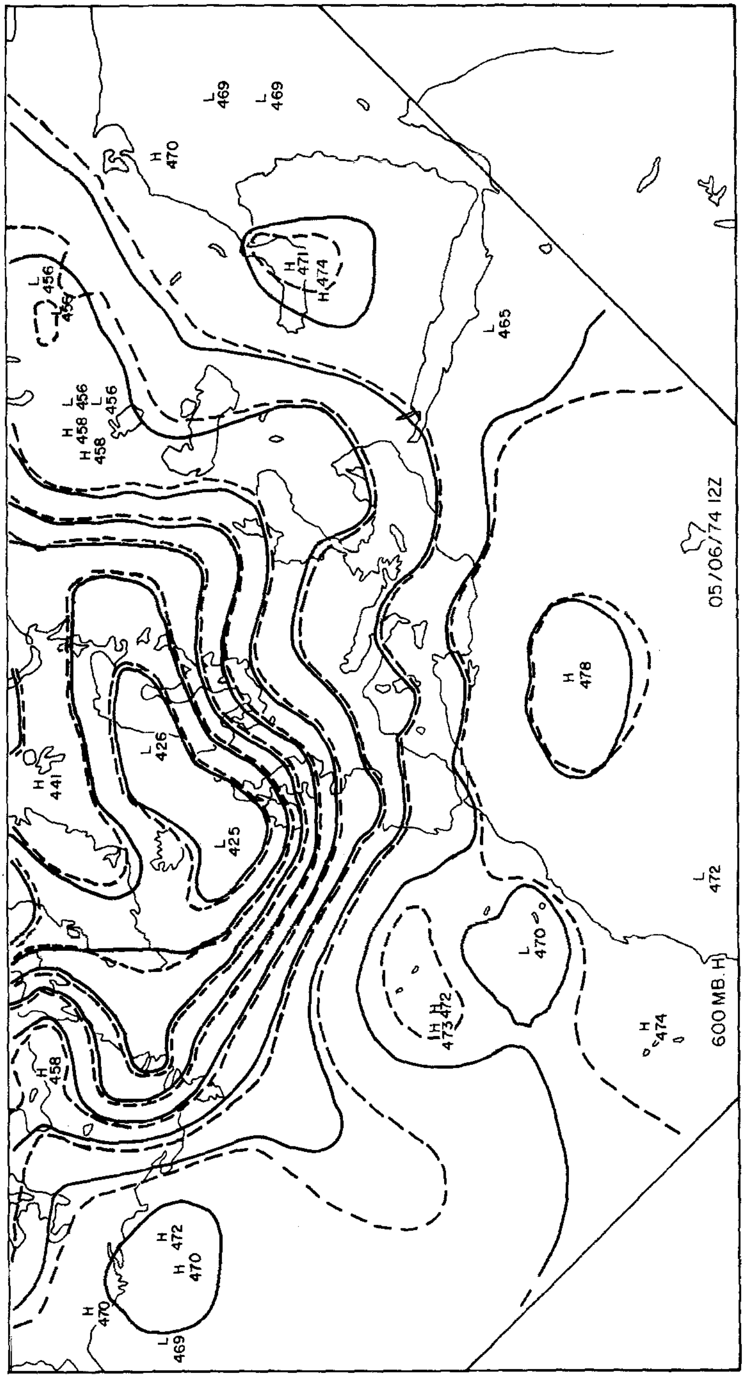

Fig. 5. 600 mb isohypse contours in dekameters for 05/06/74 12 z. Solid lines show SOR solution and dashed lines the ADI solution

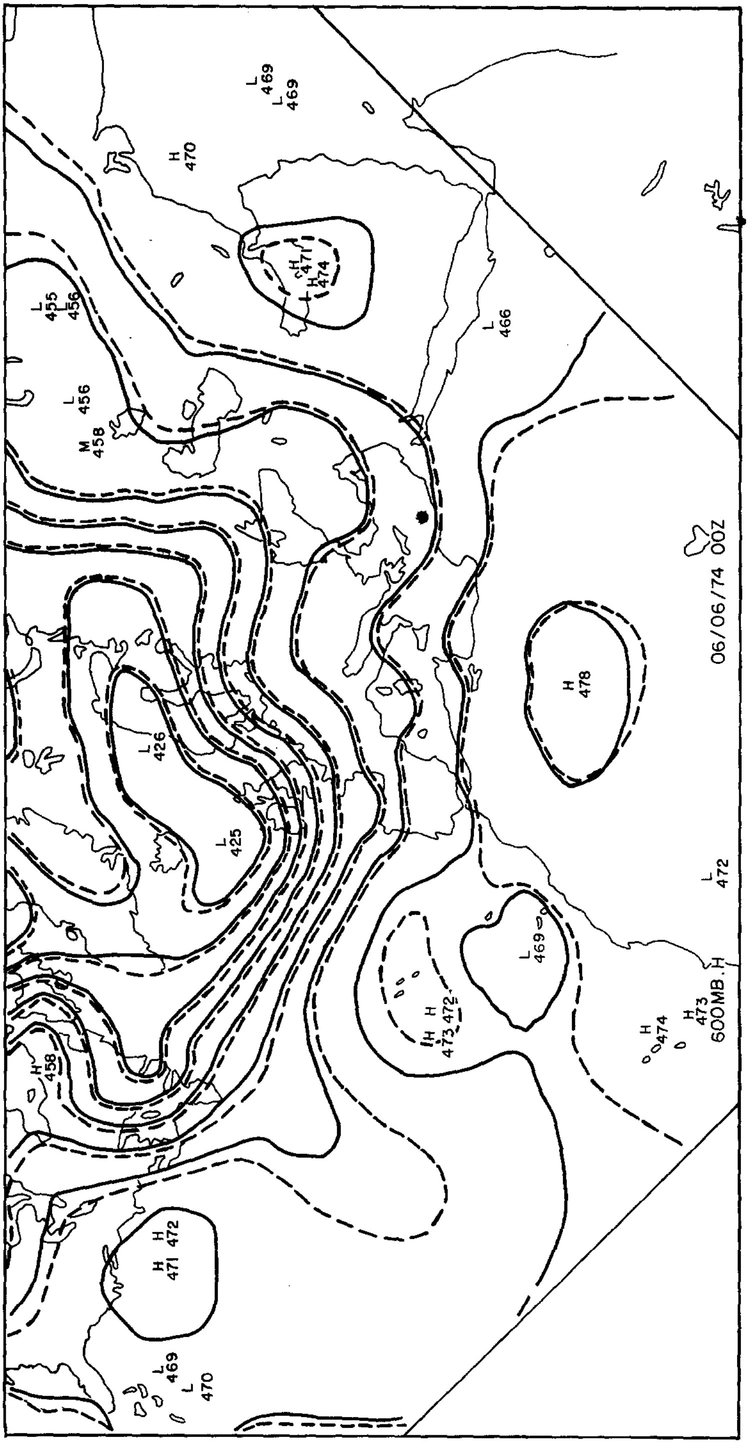

Fig. 6. 600 mb isohypse contours in dekameters for 06/06/74 00 z. Solid lines show SOR solution and dashed lines the ADI solution

5. Conclusions

Many meteorologists prefer SOR methods for complicated regions because programming is simpler. The author hopes, however, that the results derived in this paper will encourage researchers in numerical weather forecasting to employ ADI iterative methods more frequently, even for non-rectangular domains.

Acknowledgements

Thanks are extended to the NWP and Computer Group at the Israeli Meteorological Service for making available meteorological data.

References

1. Birkoff, G., Varga, R. S., Young, D.: Alternating Direction Implicit Methods. In: Advances in Computers, Vol. 3 (Alt, F. L., ed.). Academic Press 1962.
2. Crowder, H. J., Dalton, C.: Errors, in the Use of Non-Uniform Mesh Systems. J. of Computational Physics *7*, 32–45 (1971).
3. Jones, D. E.: ADI Methods. In: Bracknell's Seminar on the Iterative Solution of Linear Equations. 1963.
4. Mitchell, A. R.: Computational Methods in Partial Differential Equations, 255 p. London: John Wiley & Sons 1969.
5. Mouradoglou, A. J.: Numerical Studies on the Convergence of the Peaceman-Rachford Alternating-Direction Implicit Method. Interim Tech. Report No. 14, Computation Center, The University of Texas, Austin, Texas, June 1967.
6. Peaceman, D. W., Rachford, H. H., Jr.: The Numerical Solution of Parabolic and Elliptic Differential Equations. J. Soc. Ind. Appl. Maths. *3*, 28–41 (1955).
7. Ravdin, D.: Computer Programs for Numerical Weather Prediction. Software Dept., Elbitt Computers, Haifa (Research Report for the Israeli Meteorological Service), 1968.
8. Roache, P. J.: Computational Fluid Dynamics, 434 p. Albuquerque, N. M.: Hermosa Publishers 1972.
9. Varga, R. S.: Matrix Iterative Analysis. Englewood Cliffs, New Jersey: Prentice Hall 1962.
10. Wachpress, E. L.: Iterative Solution of Elliptic Systems. Englewood Cliffs, New Jersey: Prentice Hall 1966.
11. Wachpress, E. L.: Iterative Parameters in the Numerical Solution of Elliptic Problems. In: Symposium on the Theory of Numerical Analysis. *193*, p. 93–109. Springer 1971.
12. Windlund, O. B.: On the Rate of Convergence of an Alternating Direction Implicit Method in a Non-Commutative Case. Maths. of Computation *20*, 500–515 (1966).
13. Navon, I. M., Alperson, Z.: Application of Fourth-Order Finite Differences to a Baroclinic Model of the Atmosphere. Arch. Met. Geoph. Biokl., Ser. A *27*, 1–11 (1978).

Author's address: Dr. I. M. Navon, National Research Institute for Mathematical Sciences of the CSIR, P. O. Box 395, Pretoria 0001, South Africa.